Title
Lipidation of polyethylenimine-based polyplex increases serum stability of bioengineered RNAi agents and offers more consistent tumoral gene knockdown in vivo

Permalink
https://escholarship.org/uc/item/07s7t04m

Journal
International Journal of Pharmaceutics, 547(1-2)

ISSN
0378-5173

Authors
Zhang, Qian-Yu
Ho, Pui Yan
Tu, Mei-Juan
et al.

Publication Date
2018-08-01

DOI
10.1016/j.ijpharm.2018.06.026

Peer reviewed

Lipidation of polyethylenimine-based polyplex increases serum stability of bioengineered RNAi agents and offers more consistent tumoral gene knockdown *in vivo*

Qian-Yu Zhang[a], **Pui Yan Ho**[a], **Mei-Juan Tu**[a], **Joseph L. Jilek**[a], **Qiu-Xia Chen**[a,b], **Su Zeng**[b], and **Ai-Ming Yu**[a,*]

[a]Department of Biochemistry & Molecular Medicine, UC Davis School of Medicine, Sacramento, CA 95817, USA

[b]College of Pharmaceutical Sciences, Zhejiang University, Hangzhou, Zhejiang 310058, China

Abstract

Recently we have established a novel approach to produce bioengineered noncoding RNA agents (BERAs) in living cells that carry target RNAi molecules (e.g., siRNA and miRNA) and thus act as "prodrugs". Using GFP-siRNA-loaded BERA (BERA/GFP-siRNA) as a model molecule, this study was to define the *in vitro* and *in vivo* knockdown efficiency of BERAs delivered by liposome-polyethylenimine nanocomplex (lipopolyplex or LPP). Compared to *in vivo*-jetPEI® (IVJ-PEI) and polyplex formulations, LPP offered greater protection of BERA/GFP-siRNA against degradation by serum RNases. Particle sizes and zeta potentials of LPP nanocomplex remained stable over 28 days when stored at 4 °C. Furthermore, comparable levels of BERA/GFP-siRNA were delivered by LPP and IVJ-PEI to luciferase/GFP-expressing human SK-Hep1-Luc-GFP or A549-Luc-GFP cells, which were selectively processed into target GFP-siRNA and subsequently knocked down GFP mRNA and protein levels. In addition, LPP-carried BERA/GFP-siRNA was successfully delivered into xenograft tumors and offered more consistent knockdown of tumoral GFP mRNA level in an orthotopic hepatocellular carcinoma (HCC) SK-Hep1-Luc-GFP xenograft mouse model, while IVJ-PEI formulation showed larger variation. These findings demonstrated that lipidation of polyplexes improved serum stability of biologic RNAi molecules, which was efficiently delivered to orthotopic HCC tissues to knock down target gene expression.

Keywords

Bioengineering; RNA delivery; Lipopolyplex; siRNA; Cancer; Orthotopic HCC; Mouse model

1. Introduction

The discovery of RNA interference (RNAi) has greatly expanded the repertoire of functional RNAi molecules such as small interfering RNAs (siRNA) and microRNAs (miRNA), which mechanistically act on target messenger RNAs (mRNA) to exert posttranscriptional gene regulation and silencing (Castanotto and Rossi, 2009; Howard, 2009; Whitehead et al.,

[*]Corresponding author., aimyu@ucdavis.edu (A.-M. Yu).

2009). Theoretically, any target gene may be silenced by a properly designed siRNA molecule via RNAi machinery in cells, which signifies the great potential of RNAi based therapies for various types of diseases. Indeed there are a number of RNAi agents under clinical trials, among some of which have moved into Phase 3 trials (Burnett et al., 2011; Sullenger and Nair, 2016; Zuckerman and Davis, 2015).

The nature of RNAi molecule is critical for the outcomes of target gene silencing. Two common methods used for the production of RNAi agents are chemical synthesis and *in vitro* transcription (Dunham and Conn, 2007; Ho and Yu, 2016). Recently, there have been growing interests in developing *in vivo* approaches for the production of RNAi molecules (Duan and Yu, 2016; Ho and Yu, 2016), following the success trait of protein research and therapy that utilizes recombinant proteins produced and folded in living cells. Utilization of ribosomal RNA (rRNA) and transfer RNA (tRNA) scaffolds are able to produce a number of RNAs of interest in *E. coli* (Ponchon and Dardel, 2007; Stepanov and Fox, 2015), whereas the yields and success rates are largely variable. After the identification of stable tRNA/pre-miRNA hybrid molecules with high-level expression in common strains of bacteria (e.g., HST08) (Li et al., 2015, 2014; Wang et al., 2015) where miRNA duplexes may be substituted by target siRNA or miRNA sequences, we established a general protocol for high-yield and large-scale production of bioengineered RNAi agents (BERAs) (Chen et al., 2015). Various types of RNAi molecules have been successfully expressed and purified, including miRNAs (e.g., miR-124 and miR-27b), siRNAs (e.g., siRNA against green fluorescent protein, namely GFP-siRNA) and RNA aptamers (e.g., malachite green aptamer and VEGF aptamer) (Chen et al., 2015; Li et al., 2018). We also demonstrated that BERAs can be selectively processed into mature miRNAs or siRNAs in human cells and consequently regulate target gene expression (Chen et al., 2015; Jilek et al., 2017; Li et al., 2015, 2018; Wang et al., 2015; Zhao et al., 2016). Produced and folded in living cells, BERAs represent a novel class of biologic RNAi molecules that hold promise for research and therapy (Ho and Yu, 2016).

Nevertheless, efficient delivery of BERAs to the site of action remains a challenge. RNAs are readily degradable by the plethora of RNases in blood. To improve the metabolic stability of RNA therapeutics in serum and ensure efficient distribution to target sites, RNA molecules may be delivered by various formulations, among which cationic lipids, polymers and peptides are the most prominent (Gao and Huang, 2009; Kim et al., 2016). Polyethylenimine (PEI)-based polyplexes (complexes of nucleotides and polycations) showed excellent delivery efficiency, whereas they may pose a risk of toxicity (Lv et al., 2006). On the other hand, liposomes resemble the lipid component of cell membrane and offer great biocompatibility. Therefore, lipidation of polyplexes may reduce the toxicity of polyplexes while retaining the benefits of both carriers (Rezaee et al., 2016). Indeed recent studies have demonstrated that the resultant lipopolyplexes (LPP) show more favorable biological properties for the delivery of nucleic acid agents (Ewe et al., 2017, 2014; Schafer et al., 2010). In this study, we employed PEI-based cationic LPP to encapsulate biologic siRNA molecule, namely BERA/GFP-siRNA (Fig. 1), and defined the delivery and knockdown efficiency both *in vitro* and *in vivo*, as compared to *in vivo*-jetPEI® (IVJ-PEI).

2. Materials and methods

2.1. Materials.

1,2-dioleoyl-3-trimethylammonium-propane (DOTAP) and cholesterol were purchased from Avanti Polar Lipids (Alabaster, AL). DSPE-PEG$_{2000}$ was purchased from NOF America Corporation (White Plains, NY). Branched polyethylenimine with molecular weight 10,000 (bPEI10k) was bought from Alfa Aesar (Wardhill, MA). *In vivo*-jetPEI (IVJ-PEI) was bought from Polyplus Transfection (Illkirch, France). Lipofectamine 3000 (LF3000), TRIzol RNA isolation reagent, and BCA protein assay kit were purchased from Thermo Fisher Scientific (Waltham, MA). Direct-zol RNA MiniPrep Kit was from Zymo Research (Irvine, CA). Matrigel was purchased from Corning (Corning, NY). All other chemicals and organic solvents of analytical grade were purchased from Sigma Aldrich or Thermo Fisher Scientific.

2.2. Human cell Lines

The human HCC cell line SK-Hep1 and lung cancer cell line A549 were bought from American Type Culture Collection (Manassas, VA, USA). The luciferase and GFP-expressing SK-Hep1-Luc-GFP and A549-Luc-GFP cells were generated after transduction with pCCLc-Luc-EGFP lentiviral constructs (Vector Core, UC Davis Medical center, Sacramento CA). Cells were cultured in EMEM (SK-Hep1-Luc-GFP) and RPMI-1640 (A549-Luc-GFP) medium containing 10% fetal bovine serum (FBS, Gibco, Grand Island, NY), at 37 °C in a humidified 5% CO_2 atmosphere.

2.3. Expression and purification of BERA/GFP-siRNA

BERA/GFP-siRNA was expressed and purified as previously described (Chen et al., 2015; Li et al., 2018). Briefly, *E. coli* (strain HST08) was transformed with BERA/GFP-siRNA expressing plasmids and grown at 37 °C for 12 h. Total RNA was isolated from bacteria using Tris-HCl-saturated phenol extraction method, and target BERA/GFP-siRNA was purified by anion exchange fast protein liquid chromatography (FPLC) method using a NGC FPLC System (BioRad, Hercules, CA). Purity of BERA/GFP-siRNA (> 99%) was determined by high performance liquid chromatography (HPLC) assay (Chen et al., 2015; Li et al., 2018) using an XBridge OST C$_{18}$ column (2.1 × 50 mm, 2.5 μm particle size; Waters, Milford, MA) on a Shimadzu LC-20AD HPLC system, and RNA concentrations were quantitated with a NanoDrop 2000 Spectrophotometer (Thermo Fisher Scientific).

2.4. Preparation and characterization of polyplex and LPP Nanocomplex.

3.17 mg DOTAP and 1.75 mg cholesterol (molar ratio = 1:1) were dissolved in chloroform in a 25-mL round-bottom flask. Then the organic solvent was removed by rotary evaporation, and the thin lipid film formed at the bottom of flasks was hydrated in 1 mL DEPC-treated water using bath sonication, followed by further intermittent sonication with a Probe Sonicator (Thermo Fisher Scientific) for 100 s. The resultant liposomes were sterilized by passing through 0.22-μm sterile filter.

Polyplex was formed by mixing 300 μL of purified BERA/GFP-siRNA (200 μg/mL) and 300 μL bPEI10k solution of different concentrations (25, 50, 75 and 100 μg/mL) through

pipetting to determine the optimum ratio between RNA and PEI. Then, the mixture was stored at room temperature for 15 min. N/P ratios between PEI and RNA were calculated according to the following equation: N/P = (mass of the polymer × 330 g/mol)/(mass of the nucleic acid × 43 g/mol) (Ewe et al., 2014). BERA/GFP-siRNA-complexed IVJ-PEI was made at an N/P ratio of 8 following the manufacturer's instructions.

LPP was produced by mixing 300 μL freshly-prepared liposomes with 600 μL polyplex through vigorous pipetting. After 30 min of incubation at room temperature, 7.8 μL DSPE-PEG$_{2000}$ (10 mg/mL) was added to introduce PEGylated lipids into the complex to ensure the theoretical molar ratio of DSPE-PEG$_{2000}$ in surface lipid composition reached 2% and the mixture was incubated at 50 °C for 15 min. N/P ratios between PEI and RNA were calculated according to the following equation: N/P = (mass of DOTAP × 330 g/mol)/(mass of the nucleic acid × 698 g/mol).

The zeta potentials and particle sizes of polyplex and LPP nanocomplex were measured by dynamic light scattering (Malvern Zetasizer Nano ZS90 instrument, Malvern instruments Ltd. U. K.).

2.5. Storage and serum stability of LPP Nanocomplex.

To assess storage stability, LPP was stored at 4 °C and 150 μL of samples were taken out on different days and diluted to 1 mL for particle size and zeta potential measurement (Malvern Zetasizer Nano ZS90 instrument).

To determine stability in serum, 500 μL RNA-loaded formulations were mixed with 500 μL FBS and incubated at 37 °C (Maeda et al., 2004). 100 μL mixtures were collected at various time points and transferred into a 96-well plate to measure the transmittance at 750 nm using a microplate reader (SpectraMax M2, Molecular Devices, USA). Likewise, 100 μL of samples were subjected to total RNA isolation using TRIzol and analyzed by denaturing urea polyacrylamide (8%) gel electrophoresis (PAGE) to assess RNA integrity.

2.6. In vitro delivery of BERA/GFP-siRNA in human carcinoma Cells.

SK-Hep1-Luc-GFP or A549-Luc-GFP cells ($5 × 10^4$ cells/well) were seeded in 12-well plate and grown overnight. BERA/GFP-siRNA-loaded LPP nanocomplex was added into each well to a final concentration of 5 nM. LP3000 and IVJ-PEI formulations were included for comparison. After 72 h of treatment, cells were collected and total RNA was extracted with Trizol and Direct-zol RNA MiniPrep Kit (Zymo Research). cDNA was synthesized from 500 ng total RNA using NxGen M-MuLV reverse transcriptase (Lucigen, Middleton, WI, USA), with random hexamers or specific stem-loop primer for GFP-siRNA (5′-GTC GTA TCC AGT GCA GGG TCC GAG GTA TTC GCA CTG GAT ACG ACG GGC AC-3′). Levels of GFP-siRNA and precursor GFP-siRNA were determined by using U6 as the internal standard. Levels of GFP-mRNA were determined by using 18S as the internal standard. A forward primer 5′-GCG CGC AGT TGT ACT CCA GCT T-3′ and reverse primer 5′-GTG CAG GGT CCG AGG T-3′ were used for real-time qPCR analysis of GFP-siRNA. The forward and reverse primers for qPCR analysis of GFP mRNA were 5′-ACG TAA ACG GCC ACA AGT TC-3′ and 5′-AAG TCG TGC TGC TTC ATG TG-3′, respectively. The forward and reverse primers for 18S were 5′-GTA ACC CGT TGA ACC

CCA TT-3′ and 5′-CCA TCC AAT CGG TAG TAG CG-3′, respectively. The forward and reverse sequences for U6 were 5′-CTC GCT TCG GCA GCA CA-3′ and 5′-AAC GCT TCA CGA ATT TGC GT-3′, respectively. All real-time qPCR experiments were performed using iTaq Universal SYBR Green Supermix on a CFX96 Touch real-time PCR system (Bio-Rad, Hercules, CA, USA). Cells were treated in triplicate and assayed separately. The comparative threshold cycle (Ct) approach with the formula $2^{-\triangle\triangle Ct}$ was utilized to calculate the relative gene expression.

Live cell GFP fluorescence images were acquired with an Olympus IX81 microscope (Olympus, Center Valley, PA, USA) at 72 h post-transfection. To quantify the GFP fluorescence intensity, cells were first lysed with 1% Triton dissolved in PBS (1 mM EDTA). A 100 μL aliquot was collected for the measurement of GFP fluorescence (Excitation (Ex)/Emission (Em) = 488 nm/509 nm) on a microplate reader (SpectraMax M2, Molecular Devices, USA). The fluorescence intensity was normalized to total protein concentration in corresponding sample, which was quantitated by using BCA assay kit.

2.7. In vivo delivery of BERA/GFP-siRNA in orthotopic HCC xenograft mouse Models.

Animal protocol was approved by the Institutional Animal Care and Use Committee of University of California, Davis, and all procedures were conducted in accordance with the relevant national and international guidelines. To establish orthotopic HCC xenograft mouse models, SK-Hep1-Luc-GFP cells were first harvested, resuspended in PBS, and mixed with equal volume of Matrigel to a final concentration of 1×10^8 cells/mL. 4-week-old male athymic nude mice (The Jackson Laboratory, Bar Harbor, ME, USA) were anesthetized and an incision (~1 cm) along the Linea alba in the midline of the abdominal muscle layer was performed. Then 20 μL of SK-Hep1-Luc-GFP cells (2×10^6 cells) were injected into the left lobe of liver. Establishment of orthotopic HCC tumor model was confirmed by bioluminescent imaging using ChemiDoc™ MP Imaging System (BioRad, Hercules, CA), following the injection of D-luciferin (150 mg/kg) (BioVision, Inc. Milpitas, CA, USA).

Five weeks post-inoculation, mice were injected intravenously with either BERA/GFP-siRNA-loaded LPP or IVJ-PEI (20 μg/mice). After four consecutive treatments every other day, mice were sacrificed 6 h after the last dose. Then HCC tumors, liver and lung tissues were harvested. Total RNA was extracted in each sample using Trizol and Direct-zol RNA MiniPrep Kit (Zymo Research). GFP-siRNA levels were measured by stem-loop RT-qPCR, and GFP mRNA levels in liver tumors were determined by regular RT-qPCR assay using gene-selective primers, as described above.

2.8. Statistics Analysis

All values are mean ± SD. Statistical analysis was performed using two-tailed Student *t*-test or 1-way ANOVA (Prism, GraphPad Prism, San Diego, CA). Difference was considered as statistically significant at the levels of *P < 0.05, **P < 0.01 and ***P < 0.001.

3. Results

3.1. Preparation and characterization of LPP Nanocomplex.

Preparation of BERA/GFP-siRNA-loaded LPP is depicted in Fig. 1, where lipidation of polyplex was achieved by the introduction of cationic liposome. Particle sizes and zeta potentials of polyplex and LPP at various N/P ratios were first determined to identify optimal formulations. Our data showed that, while the zeta potential of polyplex gradually reversed from negative to positive, particle size decreased slowly with the increase of N/P ratio of PEI over RNA, indicating the compaction of RNA by PEI (Fig. 2A). Our results revealed that PEI-BERA formed a stable "core" at an N/P ratio around 2 to 2.5 while excessive PEI may be considered as "shell" at higher N/P ratios, similar as the PEI-DNA nanoparticle core (Yang et al., 2013). After the N/P ratio was set at 2, cationic liposomes were added to the slightly negatively charged polyplex (Fig. 2A). Once the N/P ratio between DOTAP and RNA reached 5, further addition of liposomes did not significantly change the particle size and zeta potential of LPP. Therefore, the final N/P ratio between DOTAP and RNA was set at 7.5, and the size of resultant LPP was 98.9 ± 3.6 nm and the zeta potential was 43.4 ± 3.1 mV. By contrast, particle size of BERA/GFP-siRNA-loaded IVJ-PEI was 140.9 ± 40.8 nm exhibiting a relatively higher batch-to-batch variation, and the zeta potential was 39.3 ± 4.4 mV.

3.2. Serum and storage stability of LPP

To determine the stability of nanoformulation under a physiologically relevant condition towards *in vivo* applications, RNA-loaded nanocomplexes were incubated with 50% FBS to mimic *in vivo* conditions (Zhang et al., 2015). Serum stability of LPP was first monitored by measuring the turbidity variance, in parallel to IVJ-PEI formulation. The transmittance values did not show significant changes over 24 h (Fig. 3A), indicating that there was no obvious aggregation for both IVJ-PEI and LPP formulations. However, urea PAGE analyses of extracted RNAs (Fig. 3B) showed that, compared to IVJ-PEI, LPP provided greater protection of BERA/GFP-siRNA against the degradation by serum RNases, which was indicated by a larger quantity of unchanged BERA/GFP-siRNA recovered from LPP after 24 h incubation. In sharp contrast, the majority of BERA/GFP-siRNA in the polyplex degraded after 2 h incubation, and naked BERA/GFP-siRNA degraded completely after 10-min incubation with serum (Fig. 3B).

Storage stability of LPP nanocomplex was further determined. Our data showed that particle sizes (around 90–100 nm) and zeta potentials (about 40–50 mV) of LPP remained unchanged over 28 days of storage at 4 °C (Fig. 3C and D), demonstrating an adequate colloidal stability. By contrast, polyplex in the absence of protection by lipids aggregated quickly, showing obvious precipitation even at 12 h after storage. This is consistent with previous reports that polyplex prepared with PEI was prone to aggregate during storage and lead to large and inactive particles (Ewe et al., 2014), as well as the need for fresh formulation using IVJ-PEI.

3.3. In vitro delivery of BERA/GFP-siRNA and knockdown of target GFP gene expression in human carcinoma cells

To assess the delivery of BERA/GFP-siRNA with different formulations, GFP-expressing SK-Hep1-Luc-GFP and A549-Luc-GFP cells were treated with BERA/GFP-siRNA-loaded Lipofectamine 3000, IVJ-PEI or LPP for 72 h. Levels of GFP-siRNA were determined by selective stem-loop reverse transcription qPCR assay, and the precursor GFP-siRNA and GFP mRNA levels were examined by regular qPCR using gene-specific primers, in addition to direct measurement of GFP fluorescence. While untreated SK-Hep1-Luc-GFP cells showed strong GFP fluorescence signals (Fig. 4A and B), BERA/GFP-siRNA treatment remarkably reduced fluorescence intensity among which Lipofectamine 3000 formulation showed the greatest suppression (75%), followed by IVJ-PEI (53%) and LPP (21%). This was associated with the reduction of GFP mRNA levels in SK-Hep1-Luc-GFP cells, to the greatest degrees by Lipofectamine 3000 (82%) followed by IVJ-PEI (37%) and LPP (22%) (Fig. 4C). Indeed both GFP-siRNA and precursor GFP-siRNA levels in SK-Hep1-Luc-GFP were sharply increased by all three formulations, to rather surprisingly comparable levels (Fig. 4D and E). Likewise, LPP was able to deliver sufficient BERA/GFP-siRNA to A549-Luc-GFP cells and effectively knocked down GFP gene expression, although to a slightly lower level than Lipofectamine 3000 and IVJ-PEI (Fig. 4F–I). These results showed that BERA/GFP-siRNA was successfully delivered by LPP nanocomplex to human carcinoma cells *in vitro*, which was selectively processed into target GFP siRNA and consequently reduced GFP expression.

3.4. In Vivo delivery of BERA/GFP-siRNA and knockdown of target GFP gene expression in orthotopic HCC mouse model

Following a pilot study showing that LPP-carried BERA/GFP-siRNA was distributable to some major organs, with the highest levels found in lungs and livers, upon systemic administration to healthy mice (Fig. S1), we established an orthotopic HCC xenograft tumor mouse model in this study by implantation of luciferase- and GFP-expressing SK-Hep1-Luc-GFP cells into the left liver lobe to critically evaluate the *in vivo* delivery efficiency to tumor tissues using LPP nanocomplex. Establishment of HCC xenograft tumor was confirmed by noninvasive bioluminescence imaging of luciferase signals (Fig. S2). Six hours after the last of a total of four doses of LPP-BERA/GFP-siRNA (i.v., every other day), mice were euthanized and lungs, healthy livers and HCC tumors were dissected. As revealed by selective stem-loop RT qPCR analyses, HCC xenograft tumor tissues showed high levels of BERA/ GFP-siRNA accumulation, which are comparable between IVJ-PEI and LPP-mediated delivery (Fig. 5A). Interestingly, while both IVJ-PEI and LPP-formulated BERA/ GFP-siRNA reduced tumoral GFP mRNA levels (by 36% and 60%, respectively), LPP nanocomplex led to a more consistent and greater degree of suppression (Fig. 5B). In addition, high levels of GFP-siRNA were also identified in lung and healthy liver tissues, and LPP seemed to deliver more RNAs into lungs than IVJ-PEI (Fig. 5C and D). Together, these results demonstrated the effectiveness of LPP-BERA/GFP-siRNA nanocomplex to knock down target gene expression in orthotopic HCC xenograft tumors.

4. Discussion

There are growing interests in developing RNA therapeutics in recent years, including antisense oligonucleotides, siRNA, miRNA and mRNA (Dong et al., 2016; He et al., 2016; Kranz et al., 2016; Peng et al., 2017; Sakurai et al., 2017; Zeng et al., 2017). In contrast to conventional RNA molecules made via chemical synthesis that introduces various and extensive artificial modifications or *in vitro* transcription that lacks necessary posttranscriptional modifications, our BERAs are produced and folded within intact living cells and should better capture the properties of cellular RNAs (Duan and Yu, 2016; Ho and Yu, 2016). In the present study, using BERA/GFP-siRNA as a model biologic RNA, we demonstrated for the first time that lipopolyplex (LPP) provided greater protection of BERAs against degradation by serum RNases than polyplex itself, and offered adequate delivery of BERA molecules to cancer cells and xenograft tumor tissues to knock down target gene expression.

Non-viral nanocarriers have emerged as favorable platforms for RNA/DNA delivery in recent years. Compared with polymeric materials with high molecular weight, lipid-based nanocarriers are of particular interest because liposomes exhibit an exceptional biocompatibility due to their lipid nature as well as the least risk of unwanted immunogenic reactions (Xue et al., 2015). Indeed most RNA drugs for systemic administration under clinical evaluations are lipid-based, including liposomes and lipid nanoparticles (LNP) (Kim et al., 2016; Sullenger and Nair, 2016; Xue et al., 2015), in addition to a number of liposomal small-molecule drugs that have already been approved by the US Food and Drug Administration (Puri et al., 2009). Among lipid-based delivery systems, LPP is a hybrid nanocomplex comprised of lipidated polyplex, and thus retains favorable properties of both liposomes and polyplex. Because of the interactions between cationic polymers and lipids, nucleic acid condensation in LPP nanocomplex usually occurs at lower carrier/nucleic acid ratio, as compared to corresponding lipoplexes, which results in a lower cytotoxicity and greater transfection efficiency (Rezaee et al., 2016). Previous studies have demonstrated that LPPs prepared with cationic liposomes are effective to deliver plasmid DNA, synthetic siRNA and *in vitro* transcribed mRNA molecules (Ewe et al., 2017; Kusumoto et al., 2013; Perche et al., 2011; Schafer et al., 2010). The present study reported an efficient delivery of unique biologic RNA molecules by LPP system and successful knockdown of target gene expression both *in vitro* and *in vivo*, where DOTAP-based liposomal outer layer was added to the negatively charged polyplex "core" to construct cationic LPP, given the fact that the electrostatic interactions between the core and the outer layer is essential for effective RNA packaging in LPP (Kusumoto et al., 2013).

Distinguished from synthetic siRNAs and *in vitro* transcribed shRNAs, BERAs produced in living cells carry just a few necessary posttranscriptional modifications (Li et al., 2015; Wang et al., 2015), showing favorable cellular stability as well as greater bioactivities than synthetic counterparts (Chen et al., 2015; Wang et al., 2015). Nevertheless, naked BERAs are also vulnerable to degradation by RNases within serum, as shown in the present study and our previous report (Wang et al., 2015), emphasizing the need for appropriate carriers. A possible reason for our finding that BERA/GFP-siRNA-loaded polyplex dissociated faster in serum than LPP is that the amount of PEI may not be enough to fully condense and protect

RNAs. Meanwhile, polyplex was inclined to aggregate during storage. After lipidation, BERA within LPP nanocomplex showed much higher metabolic stability in serum as well as storage stability, consistent with other findings on an increased colloidal stability of LPP and concomitant protection from polyplex aggregation (Ewe and Aigner, 2016; Ewe et al., 2014).

While the addition of PEGylated lipids such as DSPE-PEG$_{2000}$ may further improve the stability of LPP (Kim et al., 2003; Xia et al., 2016), it might reduce the final gene knockdown efficiency *in vitro*. Some liposomes utilized for systemic delivery of RNA therapeutics in clinical trials chose to include 1–2% of PEGylated lipids to ensure stability and retain adequate delivery efficiency (Jayaraman et al., 2012; Strumberg et al., 2012). Therefore, the molar ratio of DSPE-PEG$_{2000}$ on the liposome surface of LPP nanocomplex in this study was fixed at 2%. As reported (Kim et al., 2003; Xia et al., 2016), we found a greater metabolic and storage stability of our BERA-loaded LPP nanocomplex than polyplex and IVJ-PEI formulation, whereas a relatively lower *in vitro* knockdown efficiency in human carcinoma cells. However, it was surprising to find that LPP was more consistent and inclined to be more effective in knocking down target GFP gene expression in orthotopic HCC xenograft tumors than IVJ-PEI. A possible reason is that the higher metabolic stability of LPP-BERA nanocomplex would lead to a less variable and more favorable pharmacokinetic profile, which warrants more comprehensive investigation. Furthermore, a greater gene knockdown in tumor tissues by LPP might be related to a more efficient endosomal escape that is often identified for positively charged lipid/ peptide delivery systems. Actually, *in vitro* and *in vivo* delivery of nucleic acid molecules do not necessarily correlate (Ewe et al., 2017; Yang et al., 2013) because the model systems differ in many aspects. As a whole body system, *in vivo* xenograft tumor animal models, especially orthotopic tumor models, are more clinically relevant than cell based systems.

It is also noteworthy that pulmonary GFP-siRNA levels were quite high following systemic administration of LPP-BERA/GFP-siRNA nanocomplex into mouse models, suggesting that LPP could be employed to deliver drugs for the treatment of lung diseases. Indeed our novel RNA bioengineering technology permits large scale production of biologic RNA agents that may carry a variety of small RNAs including antisense RNAs, aptamers, miRNAs and siRNAs (Chen et al., 2015; Jilek et al., 2017; Li et al., 2015, 2018; Wang et al., 2015), whose therapeutic potentials shall be assessed by using the LPP system that was proven superior to polyplex and IVJ-PEI. In addition, the lipid surface of LPP could be modified towards a higher cellular uptake and knockdown efficiency, making it a highly tunable drug delivery system holding great promise (Ewe and Aigner, 2016; Xia et al., 2016).

5. Conclusion

In summary, novel bioengineered RNAi agents have been successfully formulated into LPP through lipidation of polyethylenimine-based polyplexes, using BERA/GFP-siRNA as a model molecule. LPP was revealed to provide greater protection of BERA/GFP-siRNA from degradation by serum RNases than polyplex or IVJ-PEI formulations, and LPP nanocomplexes were highly stable during storage at 4 °C for up to 28 days. LPP-carried BERA/GFP-siRNA was effective to knockdown target GFP expression in human carcinoma

cells *in vitro*. Furthermore, systemic administration of LPP-carried BERA/GFP-siRNA was distributable to orthotopic HCC xenograft tumors in mouse models *in vivo*, leading to a more consistent suppression of target gene expression than IVJ-PEI. These findings demonstrate that cationic lipid and polyethylenimine combined LPP offers an efficient platform for the delivery of biologic RNAi molecules to tumor tissues that may be applicable to anticancer drug development.

Supplementary Material

Refer to Web version on PubMed Central for supplementary material.

Acknowledgements

References

Burnett JC, Rossi JJ, Tiemann K, 2011 Current progress of siRNA/shRNA therapeutics in clinical trials. Biotechnol. J 6, 1130–1146. [PubMed: 21744502]

Castanotto D, Rossi JJ, 2009 The promises and pitfalls of RNA-interference-based therapeutics. Nature 457, 426–433. [PubMed: 19158789]

Chen QX, Wang WP, Zeng S, Urayama S, Yu AM, 2015 A general approach to high-yield biosynthesis of chimeric RNAs bearing various types of functional small RNAs for broad applications. Nucl. Acids Res 43, 3857–3869 gkv228. [PubMed: 25800741]

Dong YZ, Dorkin JR, Wang WH, Chang PH, Webber MJ, Tang BC, Yang J, Abutbul-Ionita I, Danino D, DeRosa F, Heartlein M, Langer R, Anderson DG, 2016 Poly(glycoamidoamine) brushes formulated nanomaterials for systemic siRNA and mRNA delivery in vivo. Nano Lett 16, 842–848. [PubMed: 26727632]

Duan Z, Yu AM, 2016 Bioengineered non-coding RNA agent (BERA) in action. Bioengineered 7, 411–417. [PubMed: 27415469]

Dunham CM, Conn GL, 2007 Recombinant RNA expression. Nat. Methods 4, 547–548. [PubMed: 17599081]

Ewe A, Aigner A, 2016 Cationic lipid-coated polyplexes (lipopolyplexes) for DNA and small RNA delivery. Methods Mol. Biol 1445, 187–200. [PubMed: 27436320]

Ewe A, Panchal O, Pinnapireddy SR, Bakowsky U, Przybylski S, Temme A, Aigner A, 2017 Liposome-polyethylenimine complexes (DPPC-PEI lipopolyplexes) for therapeutic siRNA delivery in vivo. Nanomed. Nanotechnol. Biol. Med 13, 209–218.

Ewe A, Schaper A, Barnert S, Schubert R, Temme A, Bakowsky U, Aigner A, 2014 Storage stability of optimal liposome–polyethylenimine complexes (lipopolyplexes) for DNA or siRNA delivery. Acta Biomater 10, 2663–2673. [PubMed: 24590163]

Gao K, Huang L, 2009 Nonviral methods for siRNA delivery. Mol. Pharm 6, 651–658. [PubMed: 19115957]

He H, Zheng N, Song ZY, Kim KH, Yao C, Zhang RJ, Zhang CL, Huang YH, Uckun FM, Cheng JJ, Zhang YF, Yin LC, 2016 Suppression of hepatic inflammation via systemic siRNA delivery by membrane-disruptive and endosomolytic helical polypeptide hybrid nanoparticles. Acs Nano 10, 1859–1870. [PubMed: 26811880]

Ho PY, Yu AM, 2016 Bioengineering of noncoding RNAs for research agents and therapeutics. Wiley Interdisciplinary Rev.-Rna 7, 186–197.

Howard KA, 2009 Delivery of RNA interference therapeutics using polycation-based nanoparticles. Adv. Drug Deliv. Rev 61, 710–720. [PubMed: 19356738]

Jayaraman M, Ansell SM, Mui BL, Tam YK, Chen J, Du X, Butler D, Eltepu L, Matsuda S, Narayanannair JK, 2012 Maximizing the potency of siRNA lipid nanoparticles for hepatic gene silencing in vivo. Angew. Chem. Int. Ed 51, 8529–8533.

Jilek JL, Tian Y, Yu AM, 2017 Effects of MicroRNA-34a on the pharmacokinetics of cytochrome P450 probe drugs in mice. Drug Metab. Disp 45, 512–522 dmd.116.074344.

Kim HJ, Kim A, Miyata K, Kataoka K, 2016 Recent progress in development of siRNA delivery vehicles for cancer therapy. Adv. Drug Deliv. Rev 104, 61–77. [PubMed: 27352638]

Kim JK, Choi SH, Kim CO, Park JS, Ahn WS, Kim CK, 2003 Enhancement of polyethylene glycol (PEG)-modified cationic liposome-mediated gene deliveries: effects on serum stability and transfection efficiency. J. Pharm. Pharmacol 55, 453–460. [PubMed: 12803766]

Kranz LM, Diken M, Haas H, Kreiter S, Loquai C, Reuter KC, Meng M, Fritz D, Vascotto F, Hefesha H, Grunwitz C, Vormehr M, Husemann Y, Selmi A, Kuhn AN, Buck J, Derhovanessian E, Rae R, Attig S, Diekmann J, Jabulowsky RA, Heesch S, Hassel J, Langguth P, Grabbe S, Huber C, Tureci O, Sahin U, 2016 Systemic RNA delivery to dendritic cells exploits antiviral defence for cancer immunotherapy. Nature 534, 396. [PubMed: 27281205]

Kusumoto K, Akita H, Ishitsuka T, Matsumoto Y, Nomoto T, Furukawa R, El-Sayed A, Hatakeyama H, Kajimoto K, Yamada Y, Kataoka K, Harashima H, 2013 Lipid envelope-type nanoparticle incorporating a multifunctional peptide for systemic siRNA delivery to the pulmonary endothelium. Acs Nano 7, 7534–7541. [PubMed: 23909689]

Li M-M, Addepalli B, Tu M-J, Chen Q-X, Wang W-P, Limbach PA, LaSalle JM, Zeng S, Huang M, Yu A-M, 2015 Chimeric microRNA-1291 biosynthesized efficiently in Escherichia coli is effective to reduce target gene expression in human carcinoma cells and improve chemosensitivity. Drug Metab. Dispos 43, 1129–1136. [PubMed: 25934574]

Li MM, Wang WP, Wu WJ, Huang M, Yu AM, 2014 Rapid production of novel Pre-MicroRNA agent hsa-mir-27b in Escherichia coli using recombinant RNA technology for functional studies in mammalian cells. Drug Metab. Disp 42, 1791–1795.

Li PC, Tu MJ, Ho PY, Jilek JL, Duan Z, Zhang QY, Yu AX, Yu AM, 2018 Bioengineered NRF2-siRNA is effective to interfere with NRF2 pathways and improve chemosensitivity of human cancer cells. Drug Metab. Disp 46, 2–10.

Lv HT, Zhang SB, Wang B, Cui SH, Yan J, 2006 Toxicity of cationic lipids and cationic polymers in gene delivery. J. Control. Rel 114, 100–109.

Maeda N, Takeuchi Y, Takada M, Sadzuka Y, Namba Y, Oku N, 2004 Anti-neovascular therapy by use of tumor neovasculature-targeted long-circulating liposome. J Control. Rel 100, 41–52.

Peng ZH, Xie Y, Wang Y, Li J, Oupicky D, 2017 Dual-function polymeric HPMA prodrugs for the delivery of miRNA. Mol. Pharmaceut 14, 1395–1404.

Perche F, Benvegnu T, Berchel M, Lebegue L, Pichon C, Jaffrès P-A, Midoux P, 2011 Enhancement of dendritic cells transfection in vivo and of vaccination against B16F10 melanoma with mannosylated histidylated lipopolyplexes loaded with tumor antigen messenger RNA. Nanomed. Nanotechnol. Biol. Med 7, 445–453.

Ponchon L, Dardel F, 2007 Recombinant RNA technology: the tRNA scaffold. Nat. Methods 4, 571–576. [PubMed: 17558412]

Puri A, Loomis K, Smith B, Lee JH, Yavlovich A, Heldman E, Blumenthal R, 2009 Lipid-based nanoparticles as pharmaceutical drug carriers: from concepts to clinic. Crit. Rev. Ther. Drug Carrier Syst 26, 523–580. [PubMed: 20402623]

Rezaee M, Oskuee RK, Nassirli H, Malaekeh-Nikouei B, 2016 Progress in the development of lipopolyplexes as efficient non-viral gene delivery systems. J. Control. Rel 236, 1–14.

Sakurai Y, Mizumura W, Murata M, Hada T, Yamamoto S, Ito K, Iwasaki K, Katoh T, Goto Y, Takagi A, Kohara M, Suga H, Harashima H, 2017 Efficient siRNA delivery by lipid nanoparticles modified with a nonstandard macrocyclic peptide for EpCAM-targeting. Mol. Pharmaceut 14, 3290–3298.

Schafer J, Hobel S, Bakowsky U, Aigner A, 2010 Liposome-polyethylenimine complexes for enhanced DNA and siRNA delivery. Biomaterials 31, 6892–6900. [PubMed: 20561681]

Stepanov VG, Fox GE, 2015 In vivo production of small recombinant RNAs embedded in a 5S rRNA-derived protective scaffold. Rna Scaffolds 1316, 45–65.

Strumberg D, Schultheis B, Traugott U, Vank C, Santel A, Keil O, Giese K, Kaufmann J, Drevs J, 2012 Phase I clinical development of Atu027, a siRNA formulation targeting PKN3 in patients with advanced solid tumors. Int. J. Clin. Pharmacol. Ther 50, 76. [PubMed: 22192654]

Sullenger BA, Nair S, 2016 From the RNA world to the clinic. Science 352, 1417–1420. [PubMed: 27313039]

Wang WP, Ho PY, Chen QX, Addepalli B, Limbach PA, Li MM, Wu WJ, Jilek JL, Qiu JX, Zhang HJ, Li T, Wun T, White RD, Lam KS, Yu AM, 2015 Bioengineering novel chimeric microRNA-34a for prodrug cancer therapy: high-yield expression and purification, and structural and functional characterization. J. Pharmacol. Exp. Ther 354, 131–141. [PubMed: 26022002]

Whitehead KA, Langer R, Anderson DG, 2009 Knocking down barriers: advances in siRNA delivery. Nat. Rev. Drug Discov 8, 129–138. [PubMed: 19180106]

Xia Y, Tian J, Chen X, 2016 Effect of surface properties on liposomal siRNA delivery. Biomaterials 79, 56–68. [PubMed: 26695117]

Xue HY, Guo PB, Wen WC, Wong HL, 2015 Lipid-based nanocarriers for RNA delivery. Curr. Pharm. Des 21, 3140–3147. [PubMed: 26027572]

Yang J, Hendricks W, Liu G, McCaffery JM, Kinzler KW, Huso DL, Vogelstein B, Zhou S, 2013 A nanoparticle formulation that selectively transfects metastatic tumors in mice. Proc. Natl. Acad. Sci 110, 14717–14722. [PubMed: 23959886]

Zeng Y, Zhou ZX, Fan MM, Gon T, Zhang ZR, Sun X, 2017 PEGylated cationic vectors containing a protease-sensitive peptide as a miRNA delivery system for treating breast cancer. Mol. Pharmaceut 14, 81–92.

Zhang QY, Ran R, Zhang L, Liu YY, Mei L, Zhang ZR, Gao HL, He Q, 2015 Simultaneous delivery of therapeutic antagomirs with paclitaxel for the management of metastatic tumors by a pH-responsive anti-microbial peptide-mediated liposomal delivery system. J. Control. Rel 197, 208–218.

Zhao Y, Tu M-J, Wang W-P, Qiu J-X, Yu A-X, Yu A-M, 2016 Genetically engineered pre-microRNA-34a prodrug suppresses orthotopic osteosarcoma xenograft tumor growth via the induction of apoptosis and cell cycle arrest. Sci. Rep 6.

Zuckerman JE, Davis ME, 2015 Clinical experiences with systemically administered siRNA-based therapeutics in cancer. Nat. Rev. Drug Discov 14, 843–856. [PubMed: 26567702]
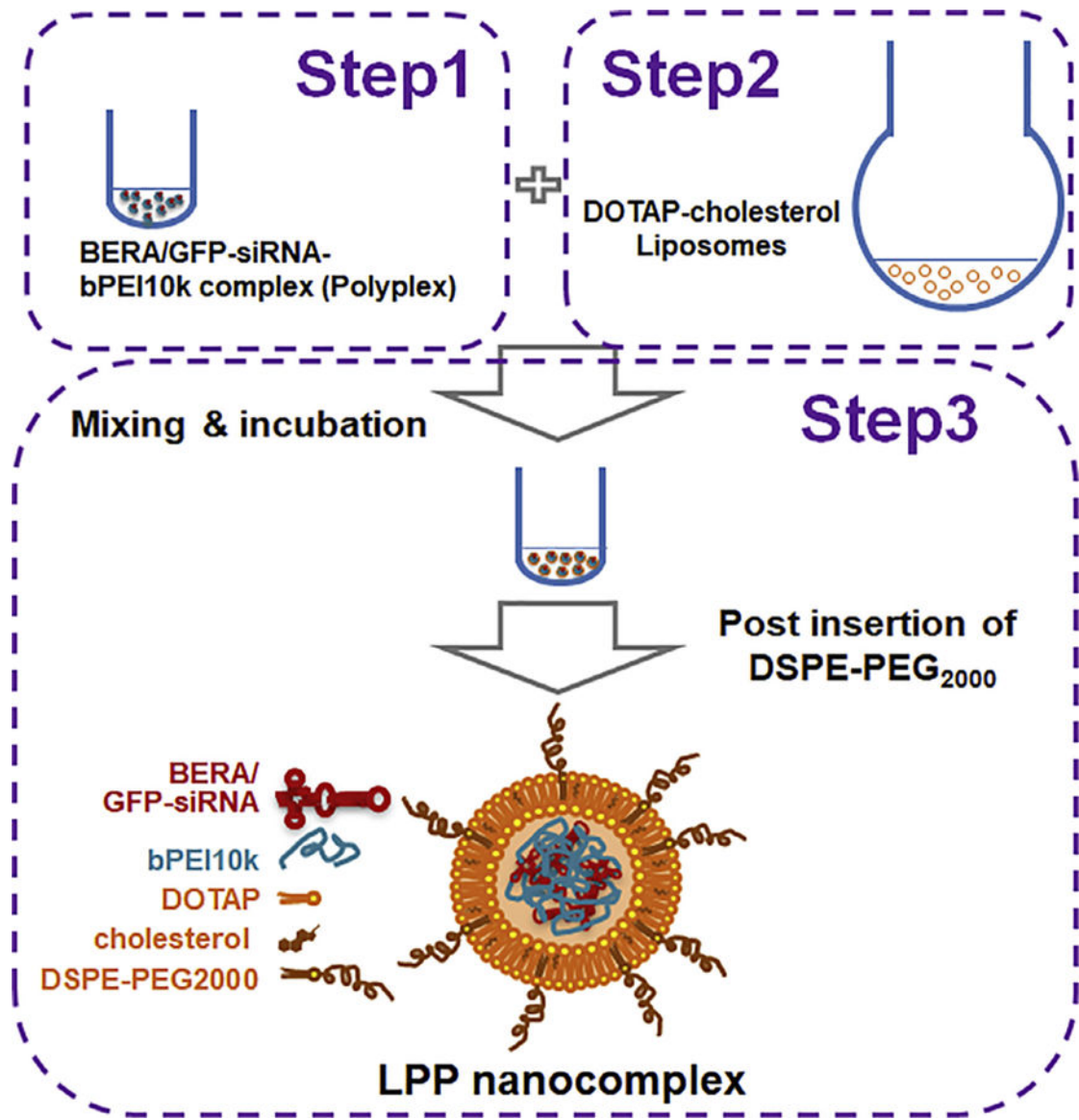
Fig. 1.
Schematic illustration of the preparation of BERA/GFP-siRNA-loaded LPP. Cationic liposome was prepared with DOTAP and cholesterol (Step 1), and polyplex was made separately by mixing BREA/GFP-siRNA and branched polyethylenimine (bPEI10k) solutions (Step 2). BERA/GFP-siRNA-loaded LPP nanocomplex was produced after the incubation of polyplex with liposomes, followed by post-insertion of DSPE-PEG$_{2000}$ (Step 3).
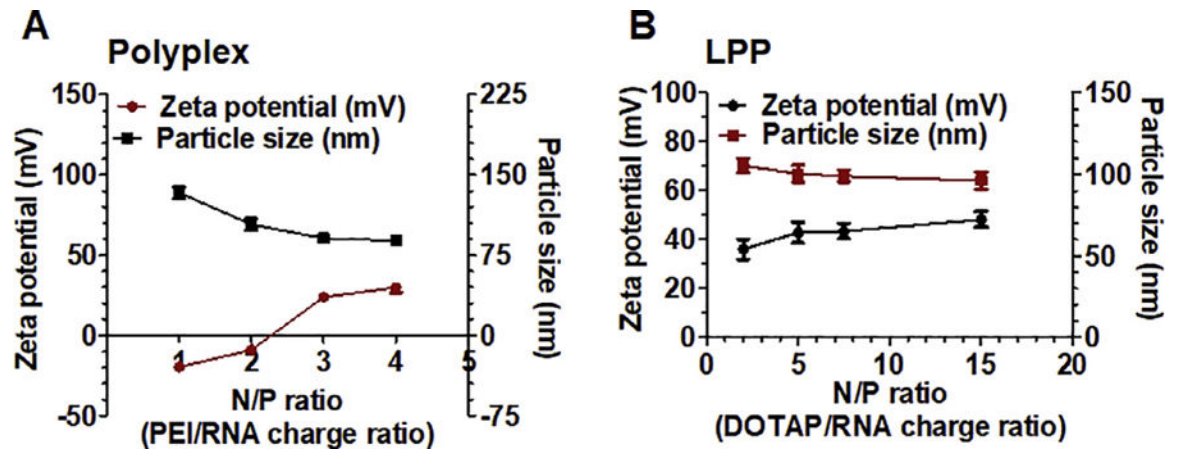
Fig. 2.
Comparison of particle size (nm) and surface Zeta potential (mV) values between polyplex (A; complex between bPEI10k and BERA/GFP-siRNA) and LPP (B; lipid coated polyplex) formulations at various N/P ratios. Values are mean ± SD (N = 3 per group).
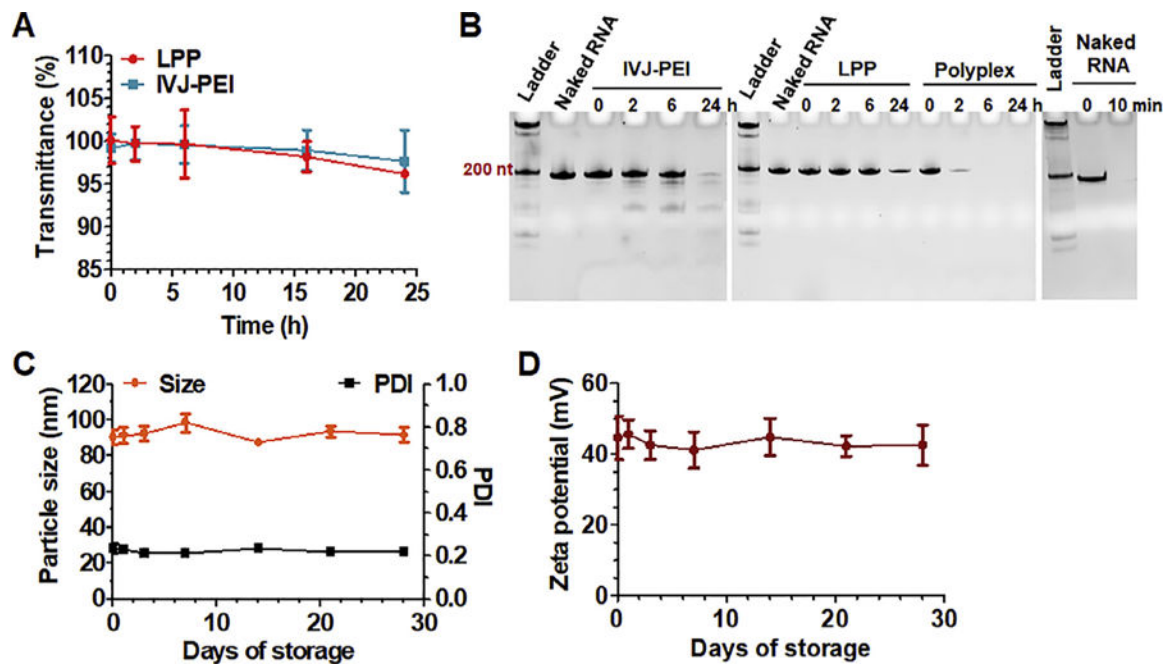
Fig. 3.

Metabolic and storage stability of biologic siRNA-loaded LPP nanocomplex. (A) Transmittance variance of BERA/GFP-siRNA-loaded LPP and IVJ-PEI in 50% FBS did not change significantly over 24 h. (B) Urea-PAGE analyses of isolated RNAs demonstrated that LPP provided better protection of BERA/GFP-siRNA molecules against degradation by serum RNases, as compared to polyplex only or IVJ-PEI formulations. Naked RNAs in the absence and presence of FBS were used as controls. 0–24 h and 0–10 min indicates the incubation times. (C) Particle sizes and polydispersity index (PDI) as well as (D) zeta potentials of BERA/GFP-siRNA-loaded LPP were unchanged over 28 days of storage at 4 °C. Values are mean ± SD (N = 3 per group).
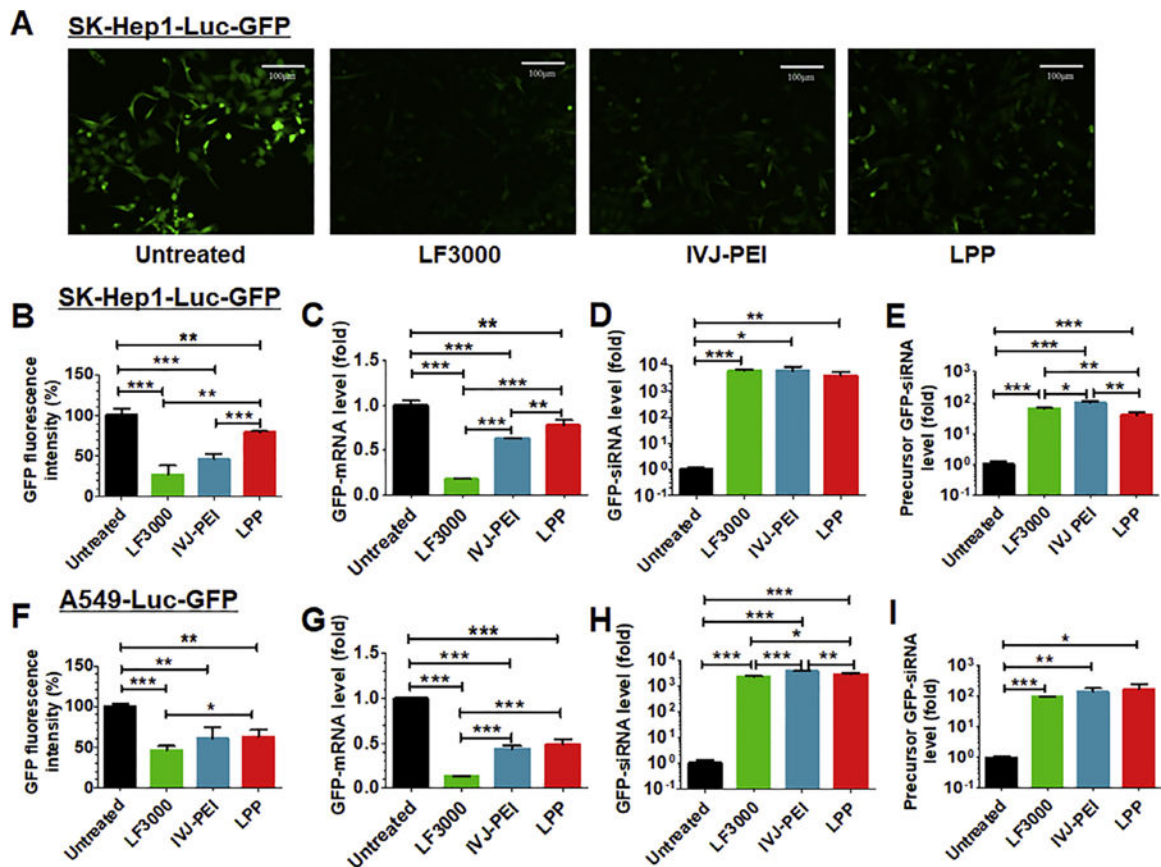
Fig. 4.
Delivery of BERA/GFP-siRNA and its knockdown efficiency in human carcinoma cells *in vitro*. (A) GFP fluorescence imaging demonstrated the knockdown of GFP by BERA/GFP-siRNA in SK-Hep1-Luc-GFP cells, delivered by Lipofectamine 3000 (LF3000), *in vivo*-jet PEI (IVJ) or LPP nanocomplex. This was further confirmed by measuring GFP fluorescence intensity (B) and mRNA levels (C) in SK-Hep1-Luc-GFP cells, attributable to the successful release of GFP-siRNA (D) from precursor GFP-siRNA levels (E). Likewise, delivery of BERA/GFP-siRNA and subsequent knockdown of GFP were shown in A549-Luc-GFP cells (F, G, H and I). Cells were treated with 5 nM BERA/GFP-siRNA for 72 h. GFP fluorescence intensity was measured at Ex/Em = 488/509 nm and RNA levels were determined by qPCR with gene specific primers. Values are mean ± SD of triplicate treatments (N = 3 per group). *P < 0.05, **P < 0.01, and ***P < 0.001.
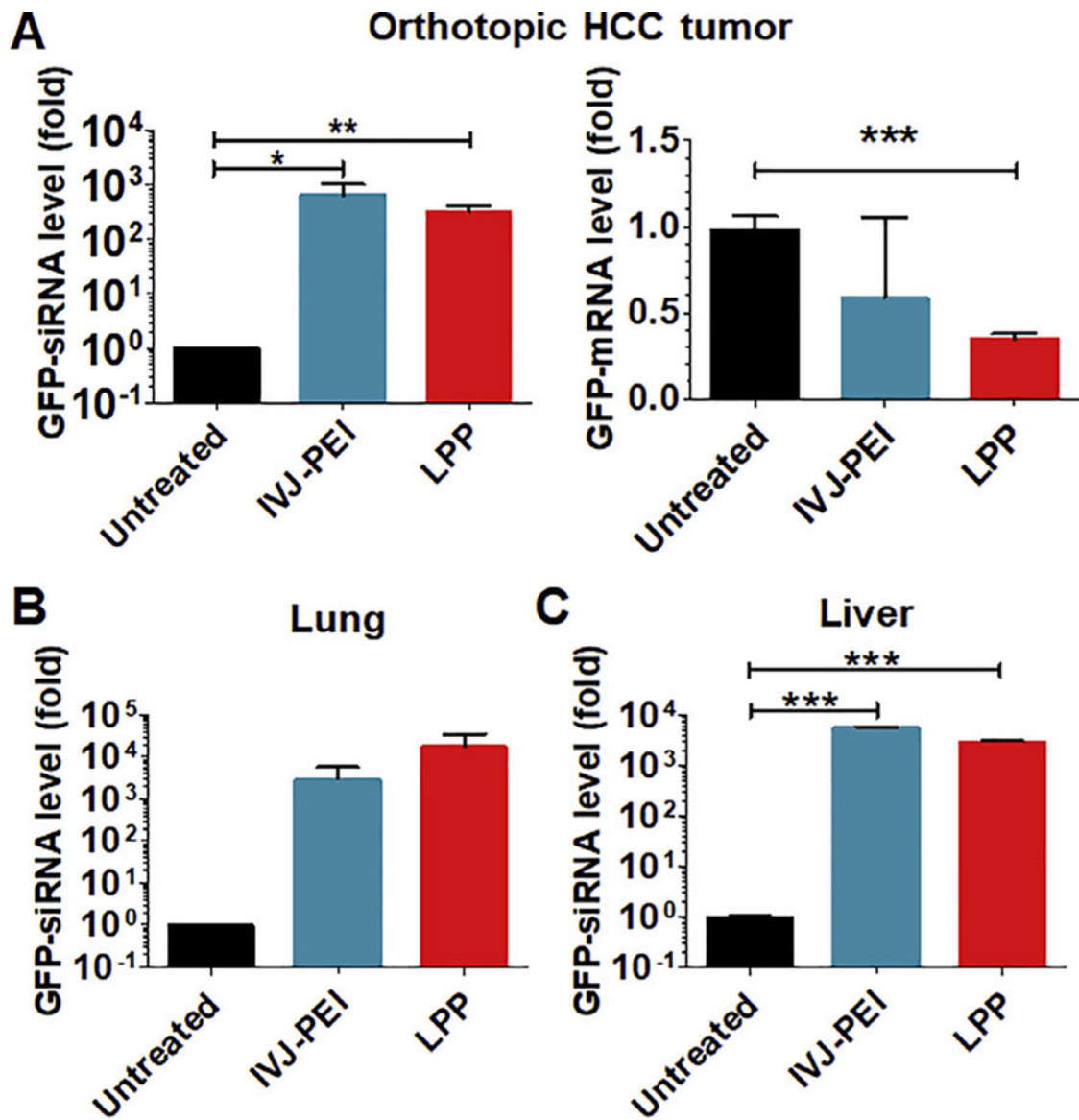
Fig. 5.
Delivery and effectiveness of BERA/GFP-siRNA in orthotopic HCC xenograft mouse models *in vivo*. (A) GFP-siRNA was successfully delivered to orthotopic HCC tumor tissues, leading to significantly lower levels of GFP mRNA. (B and C) Target siRNA molecules were also distributed to mouse lung and liver tissues. Orthotopic HCC xenograft mouse models were established after grafting SK-Hep1-Luc-GFP cells into the left liver lobe. Mice were treated i.v. with 1 mg/kg of BERA/GFP-siRNA-loaded LPP every other day for 4 times. IVJ-PEI formulated BERA/GFP-siRNA was used for comparison. GFP-siRNA and mRNA levels were determined by qPCR assays. Values are mean ± SD (N = 3 per group). $*P < 0.05$, $**P < 0.01$, and $***P < 0.001$.